

Synthesis and charge/discharge properties of cellulose derivatives carrying free radicals

Jinqing Qu^a, Fareha Zafar Khan^a, Masaharu Satoh^b, Jun Wada^c, Hiroyuki Hayashi^d, Kenji Mizoguchi^d, Toshio Masuda^{a,*}

^a Department of Polymer Chemistry, Graduate School of Engineering, Kyoto University, Katsura Campus, Kyoto 615-8510, Japan

^b Murata Manufacturing Co., Ltd., Yasu-shi, Shiga 520-2393, Japan

^c Corporate Planning Department, Nippon Kasei Chemical Co., Ltd., 1-8-8 Shinkawa, Chuo-ku, Tokyo 104-0033, Japan

^d Department of Physics Tokyo Metropolitan University, Hachioji, Tokyo 192-0397, Japan

Received 27 December 2007; received in revised form 27 January 2008; accepted 28 January 2008

Available online 2 February 2008

Abstract

Ethyl cellulose derivatives [EC-T and EC-P] and cellulose acetate derivatives [CA-T and CA-P] carrying TEMPO or PROXY radicals (TEMPO = 2,2,6,6-tetramethyl-1-piperidinyloxy, PROXY = 2,2,5,5-tetramethyl-1-pyrrolidinyloxy) were synthesized with moderate number-average molecular weights of 62 400–126 000 in 84–88% yield by the reaction of 4-carboxy-TEMPO or 3-carboxy-PROXY with residual hydroxyl group of ethyl cellulose or cellulose acetate. All the free radical-containing cellulose derivatives demonstrated reversible charge/discharge processes, whose discharge capacities were 42.8–61.1 A h/kg. In particular, the CA-T-based cell displayed two-stage discharge process, and the first-stage discharge capacity reached 29.5 A h/kg which corresponds to 74% of its theoretical value, and that of the total capacity was 61.1 A h/kg which approaches up to 153% of the theoretical value for one-electron redox reaction.

© 2008 Elsevier Ltd. All rights reserved.

Keywords: Cellulose derivatives; Charge/discharge properties; Organic radical battery

1. Introduction

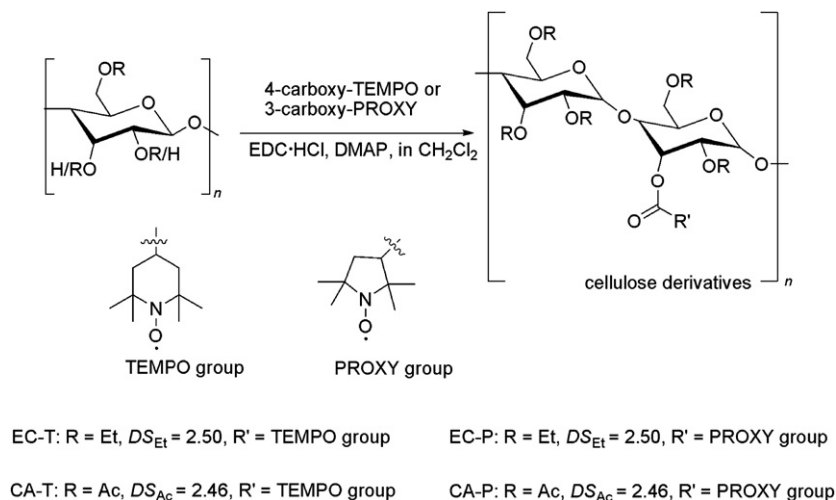
Cellulose, a sustainable and the most promising biomaterial on the earth, is incapable of being soluble in most organic solvents, while ethyl cellulose and cellulose acetate along with inheriting a lot of fascinating features of cellulose display good solubility in common organic solvents, thus finding a multitude of potential applications [1]. The past few decades have witnessed an extensive investigation on the synthesis and characterization of various cellulose derivatives, which on account of their solubility in organic solvents exhibit remarkable features of lyotropic liquid-crystal formation, chiral stationary phases for enantiomer separation, and gas separation membrane fabricability [2]. However, few efforts have been

focused on the use of cellulose derivatives as advanced materials for organic electronic applications.

TEMPO, PROXY and their derivatives are well-known stable nitroxyl radicals finding a multitude of applications in a variety of fields such as spin labels in the study of conformation and structural mobility of biological systems [3], scavengers of unstable radical species [4], and oxidizing agents [5]. Polymers carrying TEMPO and PROXY radicals have been intensively studied as subjects of electron spin resonance [6] and molecular motion [7], and frequently employed as functional materials such as polymeric stabilizers [8], oxidants of alcohols [9], and cathode-active materials in secondary batteries [10]. We have recently investigated the preparation and charge/discharge properties of several TEMPO- and PROXY-containing polyacetylenes and polynorbornenes, and revealed the attainment of theoretical discharge capacities for a number of cells fabricated with these polymers as expected from their spin density [11]. Thus far, most of the studies have been

* Corresponding author. Tel.: +81 75 383 2589; fax: +81 75 383 2590.

E-mail address: masuda@adv.polym.kyoto-u.ac.jp (T. Masuda).



Scheme 1. Synthesis and structure of cellulose derivatives.

carried out with synthetic polymers. However, there is a growing interest in natural polymers and their derivatives for practical applications from the viewpoints of biotechnology, environmental protection, and so forth. Among various natural polymers, one of the most obvious choices for these applications is cellulose, an inexhaustible natural polymeric material in the biosphere.

In the present study, we disclose the synthesis of ethyl cellulose and cellulose acetate derivatives [(EC-T, EC-P) and (CA-T, CA-P)] carrying TEMPO or PROXY radicals by the reaction of 4-carboxy-TEMPO or 3-carboxy-PROXY with the residual hydroxyl groups of organosoluble celluloses (Scheme 1), and clarifies their fundamental properties and charge/discharge characteristics of the formed polymers as cathode-active materials in an organic radical battery.

2. Experimental section

2.1. Materials

Ethyl cellulose (Fluka Biochemika, M_n : 50 000, DS_{Et} = 2.5), cellulose acetate (Aldrich, M_n : ~50 000, DS_{Ac} = 2.46), 4-carboxy-TEMPO (TCI), 3-carboxy-PROXY (TCI), *N*-(3-dimethylaminopropyl)-*N'*-ethylcarbodiimide hydrochloride (EDC·HCl; Eiweiss Chemical Corporation), and 4-dimethylaminopyridine (DMAP; Wako) were purchased and used without further purification.

2.2. Measurements

IR spectra were measured using a JASCO FT/IR-4100 spectrophotometer. Elemental analysis was conducted at the Kyoto University Elemental Analysis Center. The number- and weight-average molecular weights (M_n and M_w , respectively) of polymers were determined by gel permeation chromatography (GPC) on a JASCO Gulliver system (PU-980, CO-965, RI-930, and UV-1570) equipped with Shodex columns KF805-L×3, using tetrahydrofuran (THF) as an eluent at a flow rate of 1.0 mL/min, calibrated with polystyrene standards

at 40 °C. ESR spectra were measured on a JEOL JES-FR30 type X-band (9.48 GHz) spectrometer. The precise number of free radicals was estimated with a Quantum Design MPMS susceptometer and a home-built low-frequency ESR-NMR apparatus operated around 50 MHz [12]. Cyclic voltammograms were observed with an ALS600A-n electrochemical analyzer. The measurements were carried out with a modified ITO substrate as the working electrode coupled with a Pt plate counter electrode and an Ag/AgCl reference electrode, using a solution of the polymer (0.5 mg/mL) and tetrabutylammonium perchlorate (TBAP, 0.1 M) in CH_2Cl_2 .

2.3. Determination of degree of substitution

The degree of substitution with ethyl group (DS_{Et}) of the ethyl cellulose and with acetyl group (DS_{Ac}) of the cellulose acetate was determined by 1H NMR. The degree of substitution with TEMPO and PROXY groups in cellulose derivatives were estimated from the %N content determined by the elemental analysis data (Scheme 1). The total degrees of substitution (DS_{total}) of cellulose derivatives were calculated by the following equation:

$$DS_{total} = DS_{Et}(\text{or } DS_{Ac}) + DS_{TEMPO}(\text{or } DS_{PROXY}) \quad (1)$$

2.4. Fabrication and electrochemical measurements of the batteries using the polymers

A coin-type cell was fabricated by stacking electrodes (1.13 cm²) with porous polyolefin separator films. A cathode was formed by pressing the composites of a cellulose derivative (10 wt%), carbon fiber (80 wt%), and fluorinated polyolefin binder (10 wt%) as described in a previous paper [9a]. The cathode was set to a coin-type cell possessing a lithium metal anode. A composite solution of ethylene carbonate (30 vol%)/diethyl carbonate (70 vol%) containing 1 M of $LiPF_6$ was used as an electrolyte. Charge/discharge properties were measured at 25 °C using a computer controlled automatic battery charge

and discharge instrument (Keisokukiki, Co. Ltd., Battery Labo System BLS5500).

2.5. Theoretical capacity of polymer-based cell

The theoretical capacity (in Ah/kg) of an electroactive polymer was calculated from the molecular weight required per exchangeable unit charge in a polymer [11]:

$$C(\text{Ah/kg}) = \frac{N_{\text{Ae}}}{3600(M_{\text{w}}/1000)} \quad (2)$$

where N_{Ae} is the Faraday constant (96 487 C/mol), while M_{w} is the equivalent weight (or mass) of polymer in g, and defined as the molecular weight (molar mass) of the repeating unit of polymer divided by the number of electrons exchanged or stored by it (which may be a fractional number), or as the molecular weight of the set of repeating units exchanging (storing) one electron in polymers.

2.6. Synthesis of cellulose derivatives

EC-T was prepared as follows: 4-carboxy-TEMPO (500 mg, 2.90 mmol) was added to a solution of ethyl cellulose (1.0 g, 2.22 mmol of hydroxyl group; $\text{DS}_{\text{Et}} = 2.50$), EDC·HCl (581 mg, 3.04 mmol) and DMAP (37 mg, 0.30 mmol) in CH_2Cl_2 (30 mL) at 0 °C and the resulting mixture was stirred at room temperature for 48 h. The reaction mixture was concentrated on a rotary evaporator, and then poured into a large amount of methanol to precipitate EC-T (cf. the unreacted carboxy-TEMPO or carboxy-PROXY, and the starting cellulose derivatives were soluble in methanol) as a pale red solid, yield 85% (1.3 g). IR (KBr, cm^{-1}): 2977, 2931, 2850, 1747 (C=O), 1643, 1566, 1457 (N–O'), 1376, 1311, 1241, 1107, 918, 879, 555, 505. Anal. Calcd for $\text{C}_{32}\text{H}_{56}\text{O}_{12}\text{N}$ (Scheme 1): C, 59.33; H, 8.87; N, 2.16. Found: C, 59.41; H, 8.59; N, 2.21.

EC-P was synthesized from ethyl cellulose and 3-carboxy-PROXY in a manner similar to EC-T, pale yellow solid, yield 88%. IR (KBr, cm^{-1}): 2978, 2931, 2877, 1747 (C=O), 1651, 1566, 1458 (N–O'), 1377, 1311, 1110, 918, 879, 617, 462, 428. Anal. Calcd for $\text{C}_{31}\text{H}_{54}\text{O}_{12}\text{N}$ (Scheme 1): C, 58.75; H, 8.75; N, 2.21. Found: C, 58.12; H, 8.03; N, 2.17.

CA-T was synthesized from cellulose acetate (1.0 g, 2.23 mmol of hydroxyl group; $\text{DS}_{\text{Ac}} = 2.46$) and 4-carboxy-TEMPO in a manner similar to EC-T, pale red solid, yield 84%. IR (KBr, cm^{-1}): 2977, 2947, 1754 (C=O), 1670, 1635, 1438 (N–O'), 1373, 1234, 1164, 1049, 902, 844, 644, 601, 555, 447. Anal. Calcd for $\text{C}_{32}\text{H}_{47}\text{O}_{17}\text{N}$ (Scheme 1): C, 53.44; H, 6.73; N, 1.99. Found: C, 53.07; H, 6.30; N, 2.27.

CA-P was synthesized from cellulose acetate and 3-carboxy-PROXY in a manner similar to EC-T, pale yellow solid, yield 87%. IR (KBr, cm^{-1}): 2939, 1747(C=O), 1639, 1461 (N–O'), 1373, 1238, 1164, 1049, 902, 844, 779, 601, 482. Anal. Calcd for $\text{C}_{31}\text{H}_{45}\text{O}_{17}\text{N}$ (Scheme 1): C, 52.84; H, 6.58; N, 1.99. Found: C, 52.18; H, 6.12; N, 2.05.

3. Results and discussion

3.1. Synthesis of cellulose derivatives carrying free radicals

Cellulose derivatives carrying TEMPO or PROXY radicals were synthesized by the reaction of either 4-carboxy-TEMPO or 3-carboxy-PROXY and either ethyl cellulose or cellulose acetate, using EDC·HCl as a condensation agent and DMAP as a base (Scheme 1), and the results are summarized in Table 1. Polymeric materials with number-average molecular weights of 62 400–126 000 were obtained in 84–88% yields. Since the presence of free radicals did not allow us to measure the high-resolution NMR spectra of polymers, the polymers were identified by IR spectroscopy and elemental analysis. The spin numbers in each monomer unit in EC-T, EC-P, CA-T, and CA-P, calculated from $\text{DS}_{\text{TEMPO/PROXY}}$ and spin numbers per TEMPO or PROXY (see Table 1), were 0.75×0.50 – 1.06×0.54 .

The IR spectrum of ethyl cellulose displays a broad peak characteristic of the residual hydroxyl groups (3550 cm^{-1}), while EC-T newly showed an absorption at 1457 cm^{-1} , which is attributable to the N–O stretching of the TEMPO radical [11]. Further evidence was furnished by the presence of the peak characteristic of the carbonyl group (1747 cm^{-1}) in the IR spectrum of EC-T. According to the GPC data of EC-T (Table 1), the number-average molecular weight (M_{n}) of EC-T was estimated to be 72 200, and an increase was observed upon the incorporation of the TEMPO groups (cf. the starting ethyl cellulose: $M_{\text{n}} = 50 000$). Furthermore, the polydispersity indices ($M_{\text{w}}/M_{\text{n}} = 3.0$) of EC-T somewhat increased compared to that of ethyl cellulose ($M_{\text{w}}/M_{\text{n}} = 2.58$). These facts show that TEMPO groups have been introduced into ethyl cellulose, and the IR spectra and GPC data of EC-P, CA-T, and CA-P also indicated the incorporation of TEMPO or PROXY groups into ethyl cellulose and cellulose acetate. The DS_{Et} and DS_{Ac} were estimated to be 2.50 and 2.46, respectively, by calculating the integration ratio of methyl protons (acetyl protons) to the rest of the protons in ethyl cellulose and cellulose acetate, thus implying the presence of 0.50 and 0.54 hydroxyl groups per anhydroglucose unit, respectively [2a,b]. The degree of

Table 1
Synthesis of cellulose derivatives carrying free radicals

Sample	Yield, ^a %	M_{n} ($M_{\text{w}}/M_{\text{n}}$) ^b	DS_{TEMPO} or DS_{PROXY} ^c	DS_{total} ^d	Spin number ^e (spin/T or P)
EC-T	85	72 200 (3.0)	0.50	3.00	0.75
EC-P	88	126 000 (3.0)	0.50	3.00	0.99
CA-T	84	62 400 (2.1)	0.54	3.00	1.06
CA-P	87	65 700 (2.4)	0.54	3.00	1.06

T: TEMPO; P: PROXY.

^a Insoluble parts in methanol.

^b Determined by GPC eluted with THF; polystyrene calibration.

^c Degree of substitution of TEMPO or PROXY determined from elemental analysis (N content).

^d Total degree of substitution calculated from DS_{Et} (or DS_{Ac}) + DS_{TEMPO} (or DS_{PROXY}).

^e Average values of two independent estimations from (1) the ratio of the integrated intensity of ESR and that of broad-line ¹H NMR, measured at 50 MHz, and (2) magnetization measured with SQUID magnetometer.

substitution by TEMPO (DS_{TEMPO}) and PROXY (DS_{PROXY}) was determined by elemental analysis, and the total degrees of substitution (DS_{total}) were 3.00 for all the derivatives, indicating that the hydroxyl groups in the starting materials have been completely substituted by TEMPO or PROXY radicals. EC-T, EC-P, CA-T, and CA-P were soluble in relatively non-polar organic solvents including toluene, CHCl_3 , CH_2Cl_2 and THF, but insoluble in *n*-hexane, methanol and diethyl ether.

3.2. Physical properties of the polymers

The cyclic voltammetry (CV) curves of EC-T and CA-P are shown in Fig. 1. Reversible oxidation and reduction based on the TEMPO and PROXY radicals were observed for these polymers. EC-T exhibited an oxidation potential peak at 0.58 V versus Ag/Ag^+ , and a reduction potential peak at

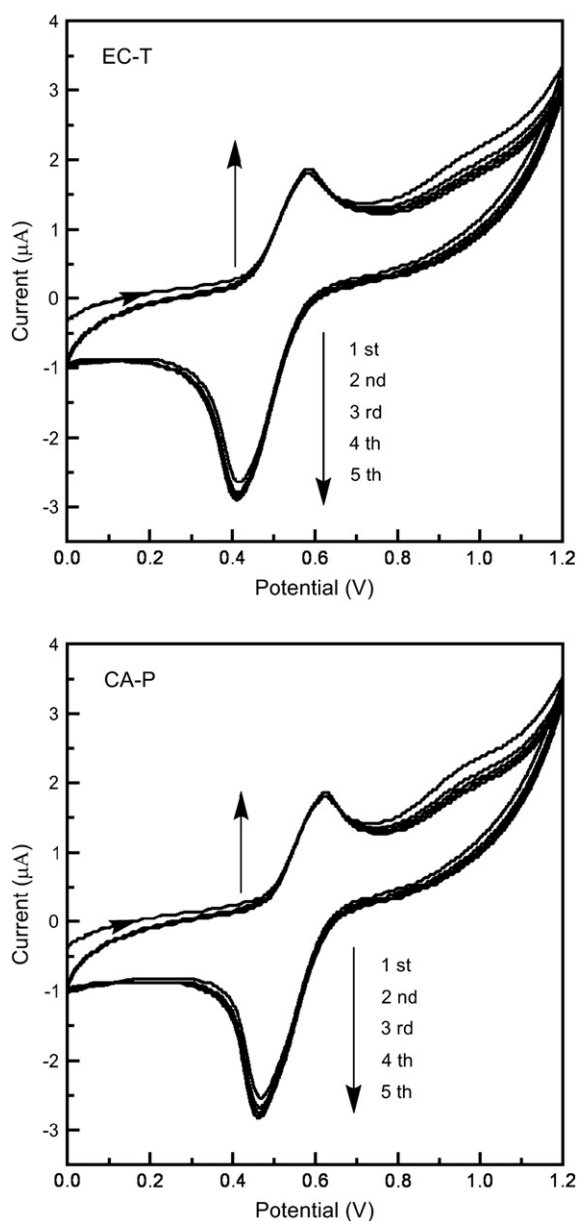


Fig. 1. Cyclic voltammograms of EC-T and CA-P measured at a scan rate of 0.01 V/s versus Ag/Ag^+ in TBAP solution.

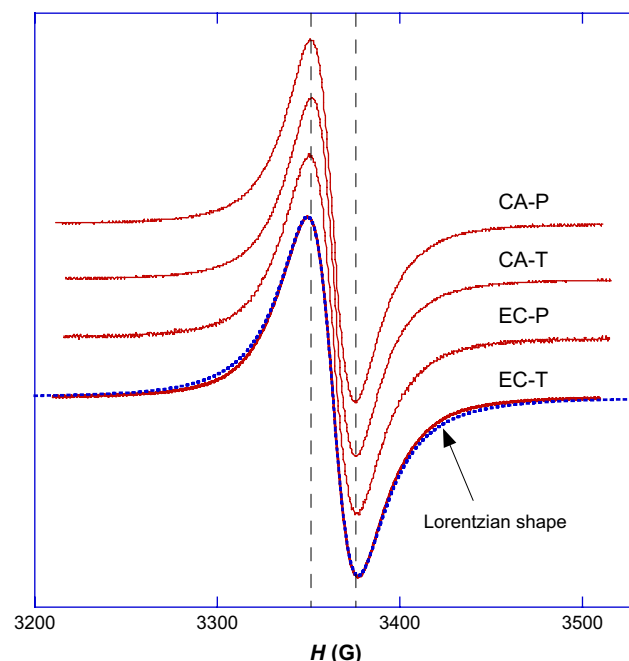


Fig. 2. ESR spectrum of EC-T, EC-P, CA-T, and CA-P in the solid state. The dotted line indicates a Lorentzian curve shape.

0.42 V versus Ag/Ag^+ at a sweep rate of 0.01 V/s, while CA-P showed the corresponding peaks at 0.62 and 0.47 V, respectively. It was observed that the distances between the oxidation and reduction potential peaks of EC-T and CA-P are 0.16 and 0.15 V, respectively, which are similar to those of other electroactive organic materials such as PTMA (ca. 0.15 V) [10]. The small gaps between the reduction and oxidation peaks generally imply large electrode reaction rates of the polymers, which suggest that these polymers will exert high power rates in the charge/discharge processes of battery under the constant battery process conditions. The oxidation and reduction peaks of EC-T and CA-P scarcely changed after five CV scans, indicating high electrochemical stability. The CV curves of EC-P and CA-T were similar to those of EC-T and CA-P.

Fig. 2 shows the derivative spectra of the electron spin resonance (ESR) of EC-T, EC-P, CA-T, and CA-P. All the ESR spectra exhibited a Lorentzian-like shape with g -factors from 2.0065 for CA-P to 2.0072 for EC-T, which are similar to that of the TEMPOL (4-hydroxy-2,2,6,6-tetramethylpiperidine-1-oxyl) radical crystals. As shown in Table 2, the ESR

Table 2
ESR data of cellulose derivatives carrying free radicals

Sample	ESR g -factor	ESR line width ^a (G)		Spin concentration ^b (10^{21} spin/g)
		~ 50 MHz	~ 9.4 GHz	
EC-T	2.0072	36.6	23.4	0.69
EC-P	2.0067	37.1	21.7	0.95
CA-T	2.0067	34.4	20.6	0.90
CA-P	2.0065	35.7	20.7	0.91

^a This frequency dependence of ESR line width is attributable to the one-dimensional spin–spin interaction along cellulose polymer chain.

^b Average values of two independent estimations from (1) the ratio of the integrated intensity of ESR and that of broad-line ^1H NMR, measured at 50 MHz, and (2) magnetization measured with SQUID magnetometer.

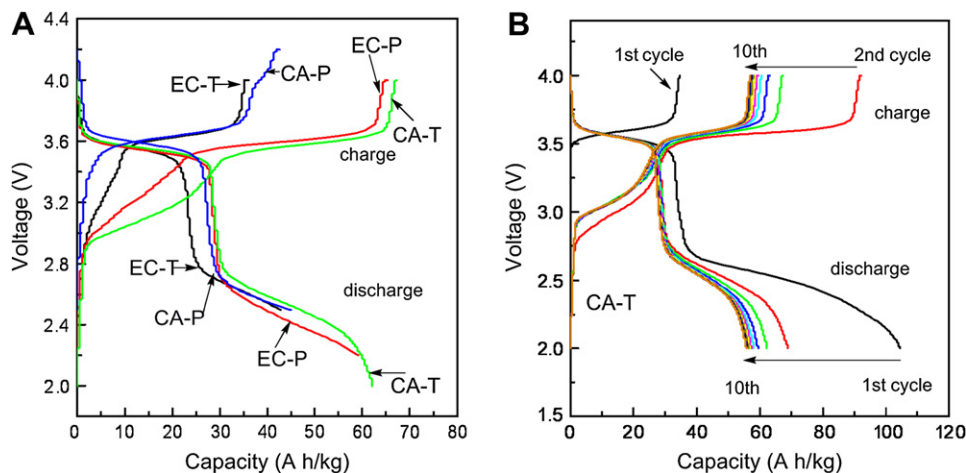


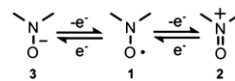
Fig. 3. Charge/discharge curves of cellulose derivatives carrying free radicals at a current density of 0.088 mA/cm^2 ($0.452\text{--}0.573 \text{ A/g}$) in the range of $2.0\text{--}4.2 \text{ V}$ cell voltage. (A) The curves of the 3rd cycle and (B) two-stage charge/discharge curves of CA-T from 1st to 10th cycle.

line widths at $\sim 50 \text{ MHz}$ were remarkably broader than that at $\sim 9.4 \text{ GHz}$, which is typical of the spin systems with one-dimensional spin–spin interaction [13]. This finding is consistent with the line shapes in Fig. 3, indicating a slight deviation from the Lorentzian curves, demonstrated by the dotted curve in Fig. 2, typical of the ESR spectra for the spin systems with three-dimensional spin–spin interaction [12].

3.3. Battery properties of the polymers

Fig. 3A illustrates the charge/discharge curves of the cells fabricated from EC-T, EC-P, CA-T, and CA-P measured in the 3rd cycle at a constant current density of 0.088 mA/cm^2 ($0.0452\text{--}0.0573 \text{ A/g}$) in the voltage range of $2.0\text{--}4.2 \text{ V}$. During the charge process of CA-T, the voltage increased progressively from 2.7 to 3.5 V in the range of $0\text{--}30 \text{ A h/kg}$ cell capacity, followed by a steady voltage plateau at about $3.5\text{--}3.7 \text{ V}$ up to a cell capacity of 65 A h/kg , and the voltage finally increased to a top cutoff voltage at 4.2 V . Similarly, during the discharge process of CA-T, the voltage quickly reduced from 4.0 to 3.7 V within $0\text{--}3 \text{ A h/kg}$ cell capacity, followed by a steady voltage plateau at about $3.7\text{--}3.4 \text{ V}$ until the capacity of 30 A h/kg , then the voltage sharply decreased to 2.7 V , followed by another slightly leaned plateau at about $2.7\text{--}2.2 \text{ V}$ up to a cell capacity of 60 A h/kg , and the voltage then again sharply decreased to a bottom cutoff voltage at 2.0 V . Thus, the discharge curve of CA-T possessed two voltage plateaus, one in the range of $3.7\text{--}3.4 \text{ V}$ and the other in the range of $2.7\text{--}2.2 \text{ V}$. The charge/discharge processes of EC-T, EC-P and CA-P resembled that of CA-T. Quite interestingly, all of the present polymers displayed clear voltage plateaus at about 3.6 V in charge/discharge curves, indicating that they can be used as cathode-active materials of organic radical batteries.

It is reasonable to assume the following for CA-T as an example (see Fig. 3B): (i) the charge process at cathode in the 1st cycle is the oxidation of TEMPO moiety **1** in the polymers to oxoammonium salt **2**, in which the charge capacity at 1st stage is about 38 A h/kg ; (ii) the discharge process in the 1st cycle is a two-stage reduction process as shown in Scheme 2, namely,



Scheme 2. The charge/discharge process of TEMPO radicals.

the first-stage reduction of salt **2** to radical **1** whose discharge capacity is 40 A h/kg , and the second-stage reduction of radical **1** to anion **3** whose discharge capacity is 66 A h/kg in the 1st cycle; (iii) the second charge process (2nd cycle) starts from **3** to finally form **2** (Scheme 2), and the charge capacity reaches about 95 A h/kg ; (iv) the charge/discharge capacities of the 3rd to 10th cycle are smaller than that of the 2nd cycle but are stabilized. It is thought that the 3rd and later cycles show the capacity inherent to CA-T, whereas some other factors such as impurities contribute to irreversible capacity in the 1st and 2nd cycles. Thus Fig. 3B clearly shows a two-stage charge/discharge process especially at the 3rd cycle and later.

Taking into account that one TEMPO moiety provides one electron in the first-stage redox process, the theoretical capacities of the cells based on EC-T, EC-P, CA-T, and CA-P are calculated to be $30.7\text{--}42.3 \text{ A h/kg}$ (Table 3). Evaluating from the values at 3.0 V in Fig. 4A, the discharge capacities in the third cycle of the cells using EC-T, EC-P, CA-T, and CA-P are determined to be $23.6\text{--}29.5 \text{ A h/kg}$ per polymer weight at a current density of 0.088 mA/cm^2 ($0.0452\text{--}0.0573 \text{ A/g}$).

Table 3
Capacity data of cellulose derivatives carrying free radicals

Sample	Theoretical capacity ^a (A h/kg)	Observed capacity (A h/kg)			Observed/theoretical capacity (%)		
		1st stage ^b	2nd stage ^c	Total	1st stage	2nd stage	Total
EC-T	30.7	23.6	19.2	42.8	77	62	139
EC-P	42.3	28.8	30.4	59.2	68	72	140
CA-T	40.1	29.5	31.6	61.1	74	81	153
CA-P	40.5	27.8	17.2	45.0	69	42	111

^a Specific charge calculated according to Ref. [11].

^b Discharge capacity in the 3rd cycle at a current density of 0.088 mA/cm^2 ($0.0452\text{--}0.0573 \text{ A/g}$), cutoff at 3.0 V .

^c Discharge capacity in the 3rd cycle at a current density of 0.088 mA/cm^2 ($0.0452\text{--}0.0573 \text{ A/g}$), cutoff at 2.0 V .

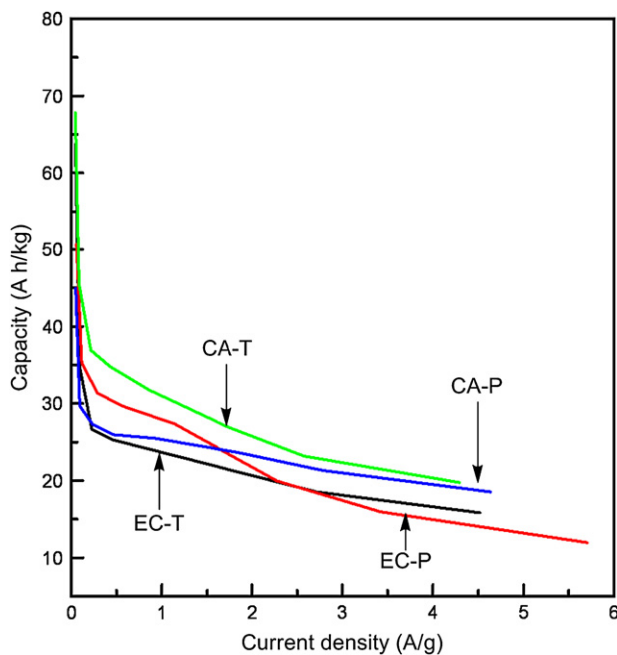


Fig. 4. Dependence of capacity on current density in EC-T, EC-P, CA-T, and CA-P.

The observed discharge capacity of CA-T was 29.5 A h/kg, which corresponds to 74% of the theoretical capacity. Moreover, evaluating from the values at 2.0 V in Fig. 3A, the discharge capacities of the cells using EC-T, EC-P, CA-T, and CA-P in the 2nd stage are determined to be 17.2–31.6 A h/kg per polymer weight at a current density of 0.088 mA/cm² (0.0452–0.0573 A/g). The observed discharge capacity of CA-T in the 2nd stage reached up to 31.6 A h/kg, and consequently the total capacity of CA-T was 61.1 A h/kg, which corresponds to 153% of the theoretical value for the one-electron redox reaction. Thus CA-T displays a large capacity thus indicating a possibility of a wide range of potential applications as a power source. The capacities of the EC-T-, EC-P-, and CA-P-based cells in the 2nd stage were 19.2, 30.4, and 17.2 A h/kg, respectively (Table 3), and were more or less lower than that of their CA-T-based counterpart. This can be ascribed to the differences not only in the spin density but also in the molecular scale structures (e.g., spatial arrangement of the TEMPO or PROXY radicals) and macroscopic aggregation states (e.g., the size and hardness of polymer powders).

Fig. 4 depicts the relationship between the capacity and current densities of EC-T, EC-P, CA-T, and CA-P. The large capacity of CA-T was maintained fairly well even though the current density was increased to 4.5 A/g. The capacity of the other polymers decreased to some extent with increasing current densities. Thus the largest capacity is available in the discharge of CA-T among the present polymers irrespective of the current densities.

Fig. 5 illustrates the cycle performance of the EC-T–CA-P/Li cells, in which charge and discharge were repeated at a current density of 0.88 mA/cm² (0.452–0.573 A/g) under the application of 2.5–4.2 V cell voltages. More than 93% of the 10th cycle capacity of the cell using CA-T was maintained

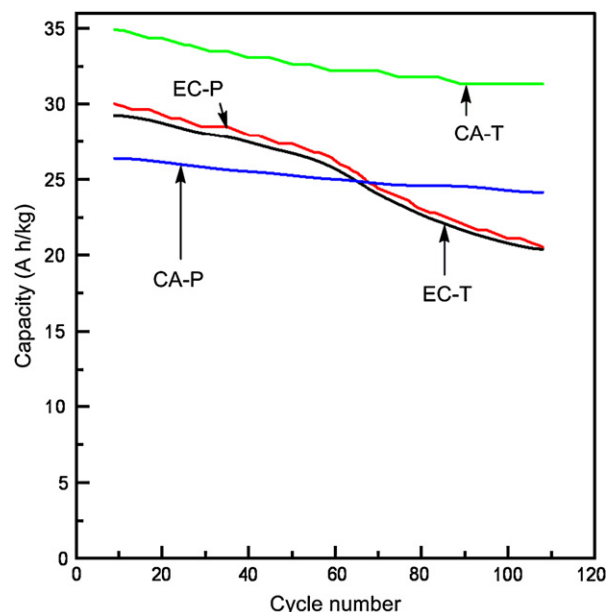


Fig. 5. Dependence of capacity on cycle number in EC-T, EC-P, CA-T, and CA-P. Charge and discharge were repeated at a current density of 0.88 mA/cm² (0.452–0.573 A/g) in the range of 2.5–4.2 V cell voltage.

after 110 cycles. The cycle-lives of EC-T- and EC-P-based cells were somewhat inferior to those of CA-T and CA-P.

4. Conclusions

We have successfully synthesized a new category of cellulose derivatives carrying TEMPO or PROXY radicals [EC-T, EC-P, CA-T, and CA-P]. All of the free radical-containing polymers demonstrated reversible charge/discharge processes, whose total capacities were 42.8–61.1 A h/kg. In particular, the total capacity of a CA-T-based cell reached 61.1 A h/kg, which corresponds to 153% of the theoretical value for one-electron redox reaction.

Acknowledgements

This research was supported in part by a grant program “Collaborative Development of Innovative Seeds” from the Japan Science and Technology Agency. Thanks are also due to the Iketani Science and Technology Foundation for financial support. Jinqing Qu acknowledges the financial support from the Ministry of Education, Culture, Sports, Science, and Technology (Monbukagakusho), Japan.

References

- [1] (a) Klemm D, Heublein B, Fink H-P, Bohn A. *Angew Chem Int Ed* 2005;44:3358–93;
- (b) Kosan B, Michels C, Meister F. *Macromol Symp* 2005;223:1–12;
- (c) Crowley MM, Schroeder B, Fredersdorf A, Obara S, Talarico M, Kucera S, et al. *Int J Pharm* 2004;269:509–22;
- (d) Zugenmaier P. *Macromol Symp* 2004;208:81–166;
- (e) Heinze T, Liebert T. *Macromol Symp* 2004;208:167–237;
- (f) Li X-G, Kresse I, Xu Z-K, Springer J. *Polymer* 2001;42:6801–10;
- (g) Barton DHR, Nakanishi K, Meth-Cohn O. *Comprehensive natural*

- products chemistry, vol. 3. Oxford: Elsevier Science; 1999;
- (h) Klemm D, Philipp B, Heinze T, Wagenknecht W. Comprehensive cellulose chemistry, vol. 1. Weinheim: Wiley-VCH; 1998. p. 2.
- [2] (a) Khan FZ, Shiotsuki M, Nishio Y, Masuda T. *Macromolecules* 2007;40:9293–303;
- (b) Morita R, Khan FZ, Sakaguchi T, Shiotsuki M, Nishio Y, Masuda T. *J Membr Sci* 2007;305:136–45;
- (c) Nakai Y, Yoshimizu H, Tsujita Y. *J Membr Sci* 2005;256:72–7;
- (d) Sato T, Shimizu T, Kasabo F, Teramoto A. *Macromolecules* 2003;36:2939–43;
- (e) Okamoto Y, Yashima E, Yamamoto C. *Top Stereochem* 2003;24:157–208;
- (f) Kubota T, Yamamoto C, Okamoto Y. *Chirality* 2003;15:77–82;
- (g) Kubota T, Yamamoto C, Okamoto Y. *J Am Chem Soc* 2000;122:4056–9;
- (h) Zugenmaier P. In: Gilbert RD, editor. *Cellulosic polymers, blends and composites*. Munich: Hanser; 1994. p. 71–94;
- (i) Gilbert RD. *ACS Symp Ser* 1990;433:259–72;
- (j) Siekmeyer M, Zugenmaier P. *Makromol Chem* 1990;191:1177–96.
- [3] (a) Columbus L, Hubbell WL. *Trends Biochem Sci* 2002;27:288–95;
- (b) Ottaviani MF, Cossu K, Turro NJ. *J Am Chem Soc* 1995;117:4387–98;
- (c) Middleton D, Reid DG, Watts A. *Biochemistry* 1995;34:7420–9;
- (d) Essman M, Hideg K, Marsh D. *Biochemistry* 1994;33:3693–7.
- [4] Bowry VW, Ingold KU. *J Am Chem Soc* 1992;114:4992–6.
- [5] (a) Adam W, Saha-Möllner CR, Ganeshpure PA. *Chem Rev* 2001;101:3499–548;
- (b) Arterburn JS. *Tetrahedron* 2001;57:9765–8.
- [6] (a) Streeter I, Wain AJ, Thompson M, Compton RG. *J Phys Chem B* 2005;109:12636–49;
- (b) Maender OW, Edward JG. *J Org Chem* 1969;34:4072–82;
- (c) Griffith H, Keana JFW, Rottschaefers S, Warlick TA. *J Am Chem Soc* 1967;89:5072.
- [7] (a) Miwa Y, Yamamoto K, Sakaguchi M, Sakai M, Tanida K, Hara S, et al. *Macromolecules* 2004;37:831–9;
- (b) Vekslis Z, Miller WG. *Macromolecules* 1977;10:686–92.
- [8] (a) Iwamoto T, Masuda H, Ishida S, Kabuto C, Kira M. *J Am Chem Soc* 2003;125:9300–1;
- (b) Petr A, Dunsch L, Koradecki D, Kutner W. *J Electroanal Chem* 1991;300:129–46.
- [9] (a) Anderson CD, Shea KJ, Rychnovsky SD. *Org Lett* 2005;7:4879–82;
- (b) Ferreira P, Phillips E, Rippon D, Tsang SC, Hayes W. *J Org Chem* 2004;69:6851–9;
- (c) Tanyeli C, Gümüş A. *Tetrahedron Lett* 2003;44:1639–42;
- (d) MacCorquodale F, Crayston JA, Walton JC, Worsfold DJ. *Tetrahedron Lett* 1990;31:771–4.
- [10] (a) Nishide H, Iwasa S, Pu YJ, Suga T, Nakahara K, Satoh M. *Electrochim Acta* 2004;50:827–31;
- (b) Nakahara K, Iwasa S, Satoh M, Morioka Y, Iriyama J, Suguro M, et al. *Chem Phys Lett* 2002;359:351–4.
- [11] (a) Katsumata T, Satoh M, Wada J, Shiotsuki M, Sanda F, Masuda T. *Macromol Rapid Commun* 2006;27:1206–11;
- (b) Qu J, Katsumata T, Satoh M, Wada J, Masuda T. *Macromolecules* 2007;40:3136–44;
- (c) Qu J, Katsumata T, Satoh M, Wada J, Igarashi J, Mizoguchi K, et al. *Chem Eur J* 2007;13:7965–73.
- [12] Capiomont A, Chion B, Lajzerowicz-Bonneteau J, Lemaire H. *J Chem Phys* 1974;60:2530–5.
- [13] (a) Mizoguchi K. *Jpn J Appl Phys* 1995;34:1–19;
- (b) Hennessy MJ, McElwee CD, Richards PM. *Phys Rev* 1973;B7:930–47.